Linking primary production, climate and land use along an urban–wildland transect: a satellite view

Yonghong Hu[1,2], Gensuo Jia[1] and Huadong Guo[3]

[1] The Key Laboratory of Regional Climate-Environment Research for Temperate East Asia, Institute of Atmospheric Physics, CAS, Beijing 100029, People's Republic of China
[2] Graduate University of the Chinese Academy of Sciences, Beijing 100049, People's Republic of China
[3] Center for Earth Observation and Digital Earth, CAS, Beijing 100190, People's Republic of China

E-mail: jiong@tea.ac.cn

Abstract
Variation of green vegetation cover influences local climate dynamics, exchange of water–heat between land and atmosphere, and hydrological processes. However, the mechanism of interaction between vegetation and local climate change in subtropical areas under climate warming and anthropogenic disturbances is poorly understood. We analyzed spatial–temporal trends of vegetation with moderate-resolution imaging spectroradiometer (MODIS) vegetation index datasets over three sections, namely urban, urban–rural fringe and wildland along an urban–wildland transect in a southern mega-city area in China from 2000–2008. The results show increased photosynthetic activity occurred in the wildland and the stable urban landscape in correspondence to the rising temperature, and a considerable decrease of vegetation activity in the urban–rural fringe area, apparently due to urban expansion. On analyzing the controlling factors of climate change and human drivers of vegetation cover change, we found that temperature contributed to vegetation growth more than precipitation and that rising temperature accelerated plant physiological activity. Meanwhile, human-induced dramatic modification of land cover, e.g. conversion of natural forest and cropland to built-up areas in the urban–rural fringe, has caused significant changes of green vegetation fraction and overall primary production, which may further influence local climate.

1. Introduction

Green vegetation cover is a critical land surface parameter that influences the hydrological cycle and water–energy exchange of the land and atmosphere (Chapin *et al* 2005, Feddema *et al* 2005, Kropelin *et al* 2008, Teixeira *et al* 2008). The monitoring of vegetation activity using time series of satellite data indicated decadal increases of vegetation growth across mid and high latitudes in correspondence to rising air temperature and probably the extended growing season (Myneni *et al* 1997). However, the response of low latitude vegetation to these conditions is not well understood, probably because vegetation photosynthesis/respiration activities are not as sensitive as northern biomes to climate warming. In addition, extensive human activities play a more important role there (Huete *et al* 2006). This is particularly evident when vegetation activities suffer more anthropogenic impacts in densely populated areas, which results in changes of land
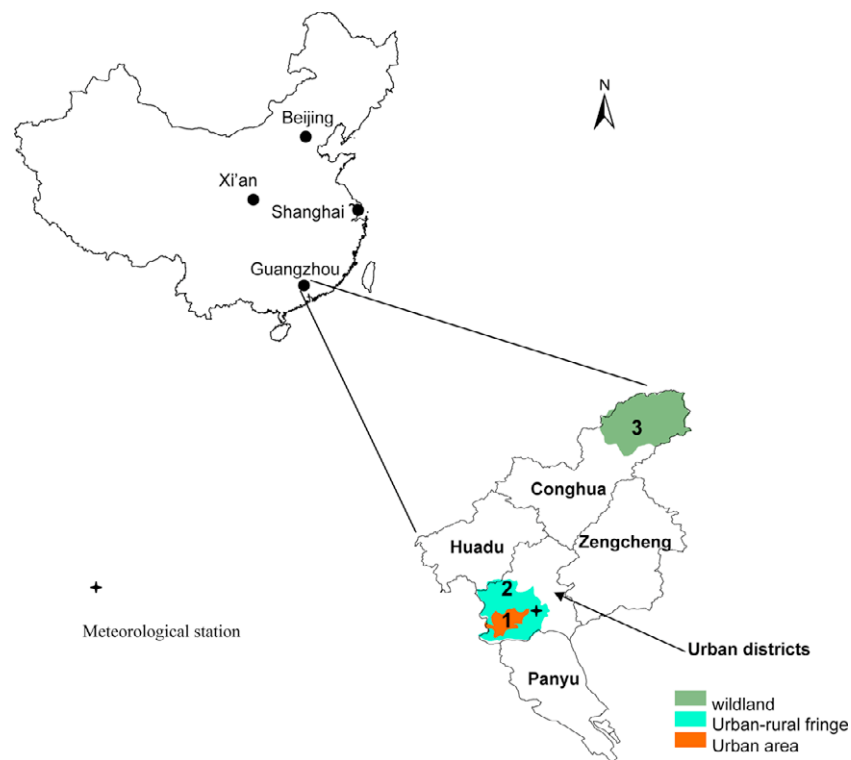
Figure 1. Location of the study area and spatial transect. Three zones, namely urban, urban–rural fringe and wildland along an urban–wildland transect, were chosen to examine primary production, climate and land use.

surface properties and local climate (Weng 2001, Kaufmann *et al* 2007, Lin *et al* 2007). Precipitation was considered to be a controlling factor that affects vegetation distribution over a large scale (Woodward and Williams 1987, Woodward *et al* 2004), while evapotranspiration of vegetation also feeds back to climate at the local, even regional, scale (Dekker *et al* 2007), especially in semiarid areas. Temperature was considered to be a controlling factor on net primary production (NPP) of various biomes (Del Grosso 2008). Urban expansion drives environmental change at multiple scales by altering land use and land cover, influencing hydrological systems and modifying biogeochemical cycles and climate (Grimm *et al* 2008). These processes quickly turn urban–rural fringe areas into concrete by eliminating natural properties step by step. Land use activities have caused a net loss of ~ 7 to 11 million km^2 of forest globally in the past 300 years (Foley *et al* 2005). Thus expansion of urban areas could greatly enhance urban thermal effects on the surrounding area and reduce the precipitation in urban areas (Trusilova *et al* 2009). The contribution of increasing vegetation cover to the lower-surface and near-surface air temperature was also reported using numerical simulation (Taha 1997). Further work is needed to examine how these driving factors influence vegetation growth and to what extent they modify land–atmosphere interactions.

Dramatic urbanization occurred in the area of southern China's mega-cities, which converted large patches of croplands and woodlands into built-up areas within a matter of a decade or even a few years. This was especially the case in Greater Guangzhou. These processes, combined with decadal changes of climate features, could have an important impact on vegetation activities along the urban–wildland transect. This study attempts to detect the response of vegetation growth to climate change and anthropogenic influence in the subtropical mega-city area by examining vegetation activities in three domains: (1) wildland mainly controlled by natural processes, (2) urban–rural fringe under extensive human disturbance with urban expansion and (3) old urban area with mostly buildings and impervious land surfaces.

2. Methods

Our case study area, the Greater Guangzhou (figure 1), was among the first areas to open their doors to the outside world after China started its economic reforms in the late 1970s and has experienced dramatic urbanization since then, with acceleration after 1990 (Weng 2001). It is located in southern China and consists of the city limit and two rural counties. The urban area on the bank of the Pearl River is surrounded by large areas of cropland and woodland (figure 2(a)). The remaining wildland (figure 2(b)) is mainly covered by secondary forest and plantation wood, usually distributed in the northeastern mountains and hills (figure 2(c)). Greater Guangzhou has a hot and humid subtropical monsoon climate that favors year-round growth of evergreen broadleaf forests, though the climate has become drier during the past 50 years, with considerable increase in temperature (figure 3(b)), in contrast to precipitation (figure 3(a)). In recent years, despite interannual fluctuations of surface humidity (figure 3(c)),
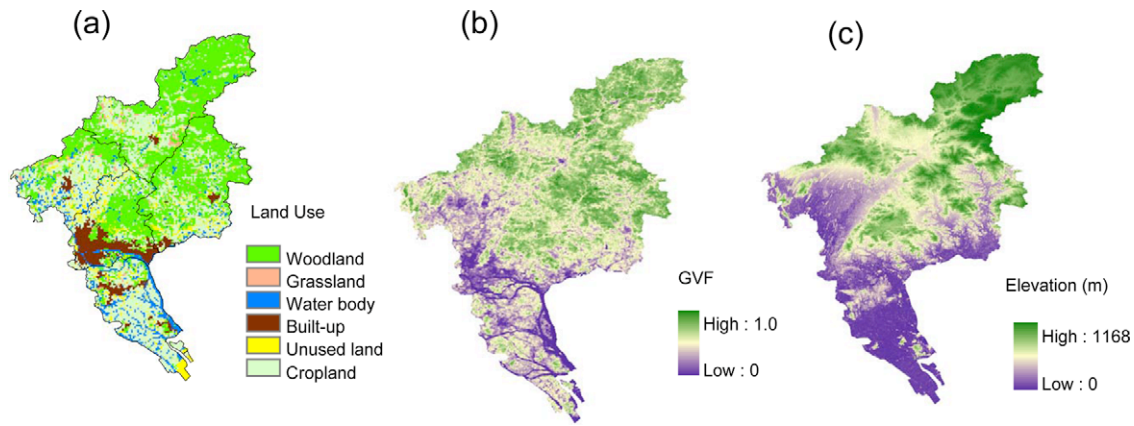
Figure 2. Spatial patterns of key factors of the study area. (a) Land use, (b) green vegetation distribution in summer, and (c) geomorphology.
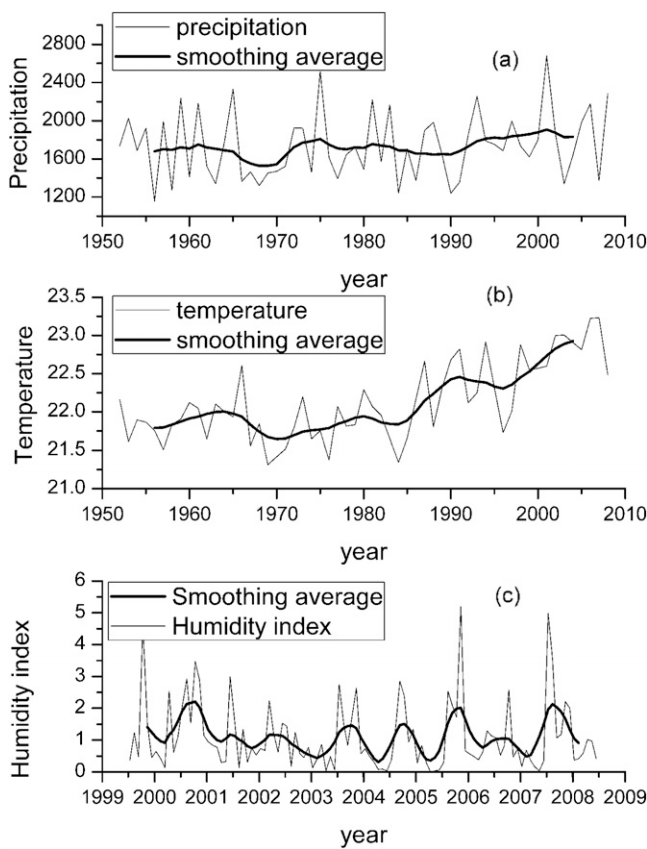
Figure 3. Annual climate trends from 1952–2008 and recent multi-year (2000–2008) surface humidity trends in Greater Guangzhou. Annual mean temperature (a) was averaged and annual total precipitation (b) was summed from daily meteorological data. Surface humidity index (c) was calculated with the Thornthwaite scheme (1948) of potential ET for land surface processes. A five-year smoothing average was performed for precipitation (a) and temperature (b) and a five-month smoothing average was performed for humidity index (c) to examine climate trends.

precipitation and soil water still meet vegetation needs without any obvious water deficit.

According to the administrative division of land use and terrain (figures 1, 2) of Greater Guangzhou in 2000,

vegetation variation under different levels of disturbance by human activities was analyzed in three zones along an urban–rural transect, including (1) an old urban area with high density building and stable environmental conditions through mostly old city downtown areas; (2) an urban–rural fringe area with rapid urban expansion and (3) wildland with forests/woodland and sparse cropland (figure 2(a)).

Vegetation indexes detect canopy greenness, canopy structure and chlorophyll content (Myneni *et al* 1995). Usually the normalized difference vegetation index (NDVI), derived from the difference of spectral reflectance in NIR and red bands of sensors, is used to analyze vegetation productivity and cover. As NDVI is constrained by the saturation phenomenon over densely vegetated area (Huete *et al* 2006), the algorithm of the enhanced vegetation index (EVI) adds the blue band and other atmospheric parameters to improve its ability to detect high biomass regions such as south China and eliminating background and atmospheric noise (Huete *et al* 2002):

$$\mathrm{EVI} = G \times \frac{\mathrm{NIR} - \mathrm{red}}{\mathrm{NIR} + C1 \times \mathrm{red} - C2 \times \mathrm{blue} + L}$$

where G is gain factor, NIR, red and blue are the surface reflectance of the corresponding band, L is the canopy background adjustment coefficient, and $C1$ and $C2$ are the coefficients for the aerosol resistance. The coefficients of $G = 2.5$, $L = 1$, $C1 = 6$ and $C2 = 7.5$ were adopted in MODIS VI.

In this study, a 16-day composite of vegetation index datasets (spatial resolution: 250 m), an 8-day composite of gross primary production (GPP) datasets (spatial resolution: 1 km) and an 8-day composite of the fraction of photosynthetically active radiation (fPAR) (400–700 nm) datasets (spatial resolution: 1 km) from the Terra Moderate Resolution Imaging Spectrometer (MODIS) sensor over the study area from 2000 to 2008 were selected to examine the annual and seasonal trends of vegetation change. fPAR is expressed as the fraction of the incoming radiation received by the land surface, which was used to quantify the photosynthetically active radiation absorbed by plants. The time series of the datasets used in this study covered February 2000 to December 2008. These datasets (a collection

of five) were developed by MODIS land teams with full consideration of atmosphere correction, cloud filter and viewing geometry (http://modis-land.gsfc.nasa.gov). Annual trends of vegetation were derived from temporally and spatially averaged EVI and GPP datasets along the transect, while the seasonal trends were derived by spatially averaged seasonal maximum values with the maximum value composite (MVC) method. The MVC method was developed to choose the maximum NDVI value during a given composite period to reduce cloud contamination, which assumes that the vegetation growth is relatively stable over this period. The traditional meteorological definition of seasons was used in considering MAM (March, April and May) as spring, JJA (June, July and August) as summer, SON (September, October and November) as autumn, and DJF (December, January and February) as winter.

In order to quantify the vegetation growth influenced by historical human activities, we examined the patterns of anthropogenic influence on vegetation over three zones along an urban–wildland transect. The EVI in JJA 2000 was derived with the MVC method to compare with land use in 2000 over the study area to analyze the anthropogenic impact on vegetation activity. Here we used the fraction of built-up area in 2000 land use raster datasets as the indicator for the intensity of human activity, by calculating the percentage of built-up fraction along the three zones and the change extension of built-up areas in the last two decades in each zone. Statistical values of EVI for each land use category were used to examine the vegetation variation among corresponding land surface conditions influenced by human activity.

Annual trends of climate change over the study area were derived from averaged daily meteorological data (temperature and precipitation) from the Guangzhou station from 1952–2008. Surface humidity index (Thornthwaite 1948, Pereira and Pruitt 2004) was used to examine the response of vegetation to different water and heat conditions in the three zones. The index was calculated from monthly temperature and precipitation data from 2000–2008 as follows:

$$H = \begin{cases} \dfrac{P}{16\,(10T/I)^{\alpha}} & 0 \leqslant T \leqslant 26 \\[2mm] \dfrac{P}{-415.85 + 42.24T - 0.43T^2} & T > 26 \end{cases}$$

where H is surface humidity index, P is monthly total precipitation (mm), T is monthly mean temperature (°C), I is surface thermal index and the exponent α is a function of I (see Thornthwaite 1948). This method defined surface humidity conditions by comparing monthly total precipitation (P) with potential evapotranspiration, which is considered to be a function of temperature and surface thermal index (Pereira and Pruitt 2004).

3. Results and discussion

3.1. Vegetation greenness along the urban–rural transect

In general, annual trends of vegetation along the urban–wildland transect (figures 4(a), (b) and (c)) were quite different
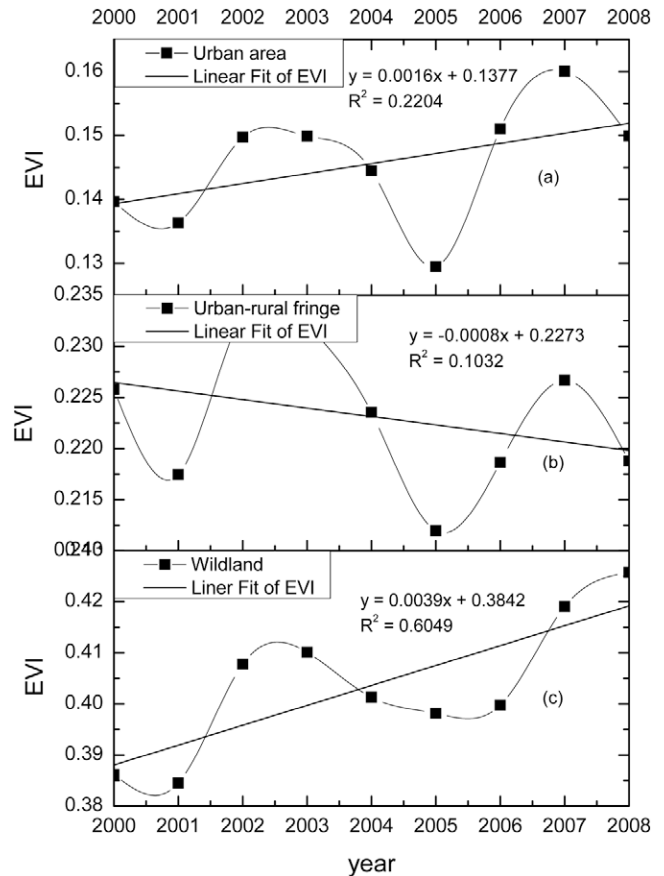

Figure 4. The annual trends of EVI along the urban–wildland transect. (a) urban, (b) urban–rural fringe and (c) wildland from 2000–2008 in Greater Guangzhou. The time series was spatially/temporally averaged from MODIS EVI datasets.

from one zone to another. Increased vegetation activity occurred in natural land and urban areas, while vegetation in the urban–rural fringe area decreased. Linear temporal trends of the EVI by linear regression from 2000–2008 indicated that the EVI in natural land and urban areas increased by 8.04% and 9.18%, while in the urban–rural fringe area it decreased by 2.83%. The time series also showed obvious EVI differences among the three zones along the transect, where natural land had a greater fraction of green vegetation cover than the fringe and urban areas by 0.13 (std 0.013) and 0.25 (std 0.009). EVI fluctuations in the study period showed similar patterns over the three zones along the transect, i.e. synchronized years of high and low values.

We further examined the patterns of seasonal trends of EVI at 250 m resolution from 2000–2008 in the study area (figure 5). All pixels were spatially aggregated and temporally averaged for each season, and then fitted with linear least squares to detect the spatial pattern of vegetation greening. Pixels with the highest EVI reduction (blue) during the study period area are noteworthy in the urban–rural fringe area, particularly at the eastern and northern sides of the city area. EVI increases are also observed over some areas in southern Conghua and eastern Zengcheng.

As expected, the complex changes of land surface over the study area are due to physical and anthropogenic impacts. The
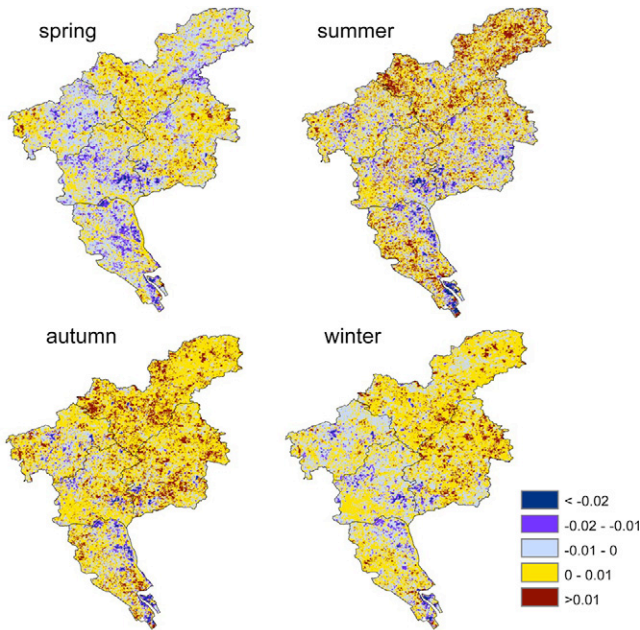
Figure 5. Spatial patterns of seasonal EVI trends from 2000–2008 during each season in Greater Guangzhou.

patterns of seasonal EVI trends showed combined signals of crop cultivation and ecological succession of young secondary forests recovered within decades. In zone 3, strengthened EVI

information was observed over all seasons except spring as the physiological activity of natural forest in spring would be stressed by less precipitation (decreased by 7%) and lower temperature (decreased by 2%) over the study period, as demonstrated by seasonal meteorological records. In contrast to spring, summer vegetation shows the greatest increase in intensity over the wildland zone, most likely because: (1) natural forest made a greater contribution to canopy structure and primary production and (2) vegetation growth was intensified by hotter temperatures in summer (increased by 0.2%) and increasing global CO_2 concentration (Doney and Schimel 2007). On the other hand, reduced vegetation activity in the urban–rural fringe are largely induced by anthropogenic modification of land surface conditions, i.e. replacing vegetation cover of woodland and crops with concrete. In the urban zone, urban vegetation was also strengthened over the period because it is more influenced by human management, which will ensure its water and nutrient supply. The primary production of this urban area is higher than from the city area found in other case studies due to water supply (Buyantuyev and Wu 2009).

3.2. Response of natural vegetation to climate

First, we examined the statistical character of the response of vegetation greenness to temperature and precipitation along the urban–rural transect (figure 6). Monthly EVI and GPP
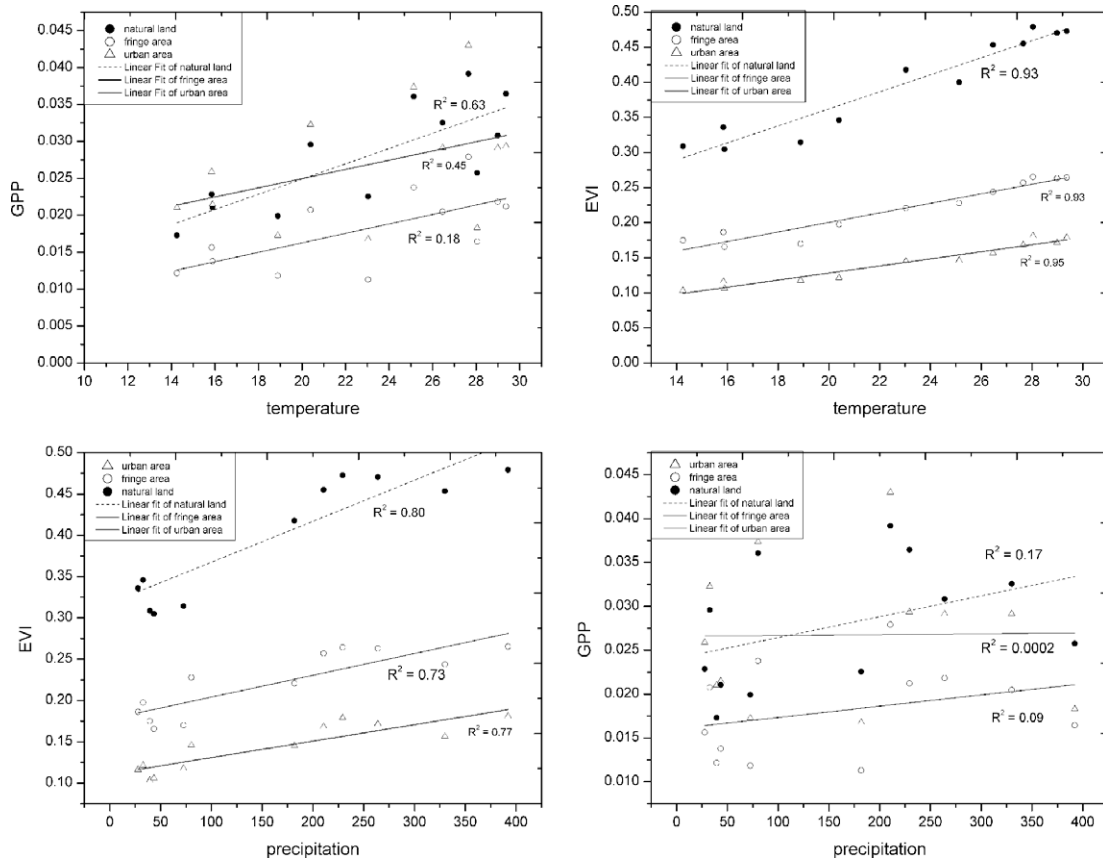
Figure 6. The response of vegetation greenness to temperature and precipitation along the urban–wildland transect from 2000–2008 in the study area. The EVI and GPP were monthly averaged with the monthly MODIS datasets from 2001–2008. Temperature and precipitation were monthly averaged from daily meteorological records.
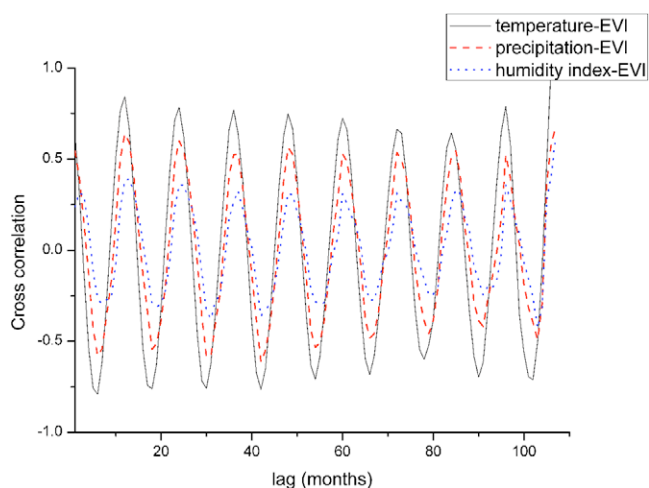
Figure 7. Cross-correlation function for EVI versus lagged temperature and precipitation.

across the three zones were averaged from 2000–2008 and meteorological data were averaged from daily meteorological records. A positive correlation was identified between EVI and climate index through the three zones and temperature has a better regression coefficient with EVI than precipitation (see R^2 values in figure 6), which indicated that the response of vegetation growth to temperature is the main control process. At the macroscale, net primary production (NPP) and net ecosystem production (NEP) increase under conditions of CO_2 increase and climate change simulated by GCM (Cao and Woodward 1998). However, the mechanism made it complicated to derive the detailed process due to the composite information from natural and anthropogenic responses. The microscale disassembles the mixed information and helps the understanding of these processes.

One site covered by secondary forest was chosen to examine the response of natural vegetation to climate. It is a relatively homogeneous 200 ha evergreen broadleaf forest located in the Liuxihe River Wild Park (in the wildland zone, see www.lxhpark.cn/). We chose pixels in a 1 km square box area within the park to examine vegetation variation under natural conditions. Cross-correlograms of monthly temperature, precipitation and EVI were calculated to examine the similarity of the time series. The lags of temperature and precipitation were considered as the lead variable for EVI variation.

Natural vegetation is one of the important response components of land surface to climate change (Braswell *et al* 1997). Figure 7 shows the cross-correlation function of EVI versus lagged temperature, precipitation and humidity index. The periodic behavior of all three variables (temperature, precipitation and EVI) autocorrelations was observed and temperature led the other variables considerably, which shows temperature was the controlling ecological factor for vegetation greenness in contrast to precipitation. Further, the lower humidity index autocorrelation shows that there was no obvious water deficit over the period. The seasonal growth of natural vegetation in each year was periodic and more related to the fluctuation of climate.
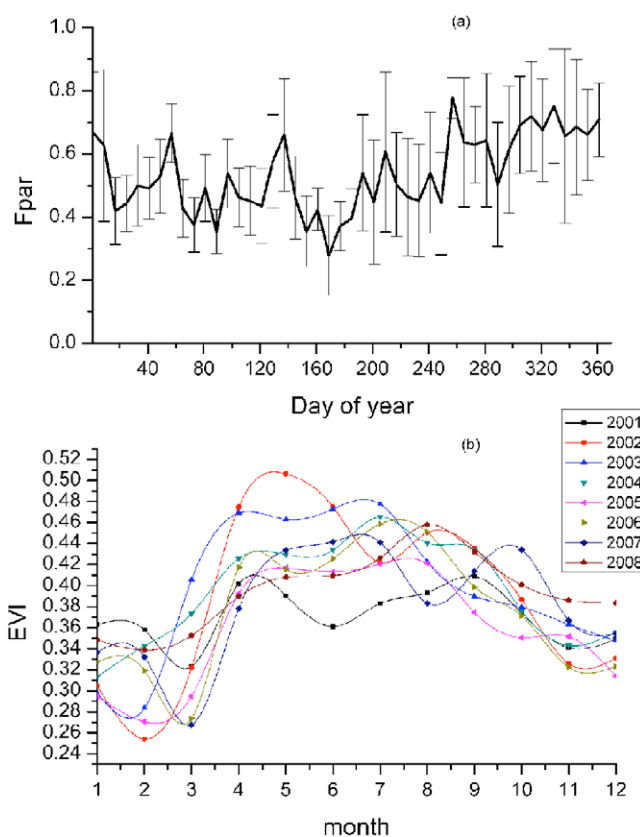
Figure 8. The seasonal trends of EVI in the wildland zone from 2000–2008 (b) and its corresponding fraction of photosynthetic radiation (a) derived and monthly averaged from MODIS fPAR datasets in the same period.

Two peaks of vegetation greenness, one occurring in mid spring (April) and another in late summer (August), were clearly identified each year over the homogeneous forest patch (figure 8(b)) in this period. This dual-peak pattern may be attributed to the 2–3 month long continuous cloudy season, that brings a much lower fraction of photosynthetically active radiation to the forest. This is because (1) cloud frequently appeared in summer in the study area to reflect, absorb and distribute the sunlight. In particular in the forest area, high evaporation levels would release more biogenic volatile organic compounds (BVOCs) as condensation nuclei to form cloud or fog. (2) Shortwave radiation (the main component of fPAR) was also reflected and absorbed by aerosols formed by BVOC. (3) MODIS EVI datasets compiled over 8 days may be fractionally contaminated by cloud. The statistical character of fPAR (figure 8(a)) from 2000–2008 showed also that there are two peaks at mid spring and late summer, as for vegetation greenness. Unlike the results of the macroscale and long term results from GCM and satellite (Braswell *et al* 1997, Cao and Woodward 1998), understanding of vegetation variation for the analysis of more complicated physiological processes in the local scale was limited by environmental factors and extreme atmospheric phenomena, such as water depression of long term rainy day or aridity, NPP decrease by fertilization saturation of CO_2 (Cao and Woodward 1998) and a decrease of the physiological activity level caused by air pollution.
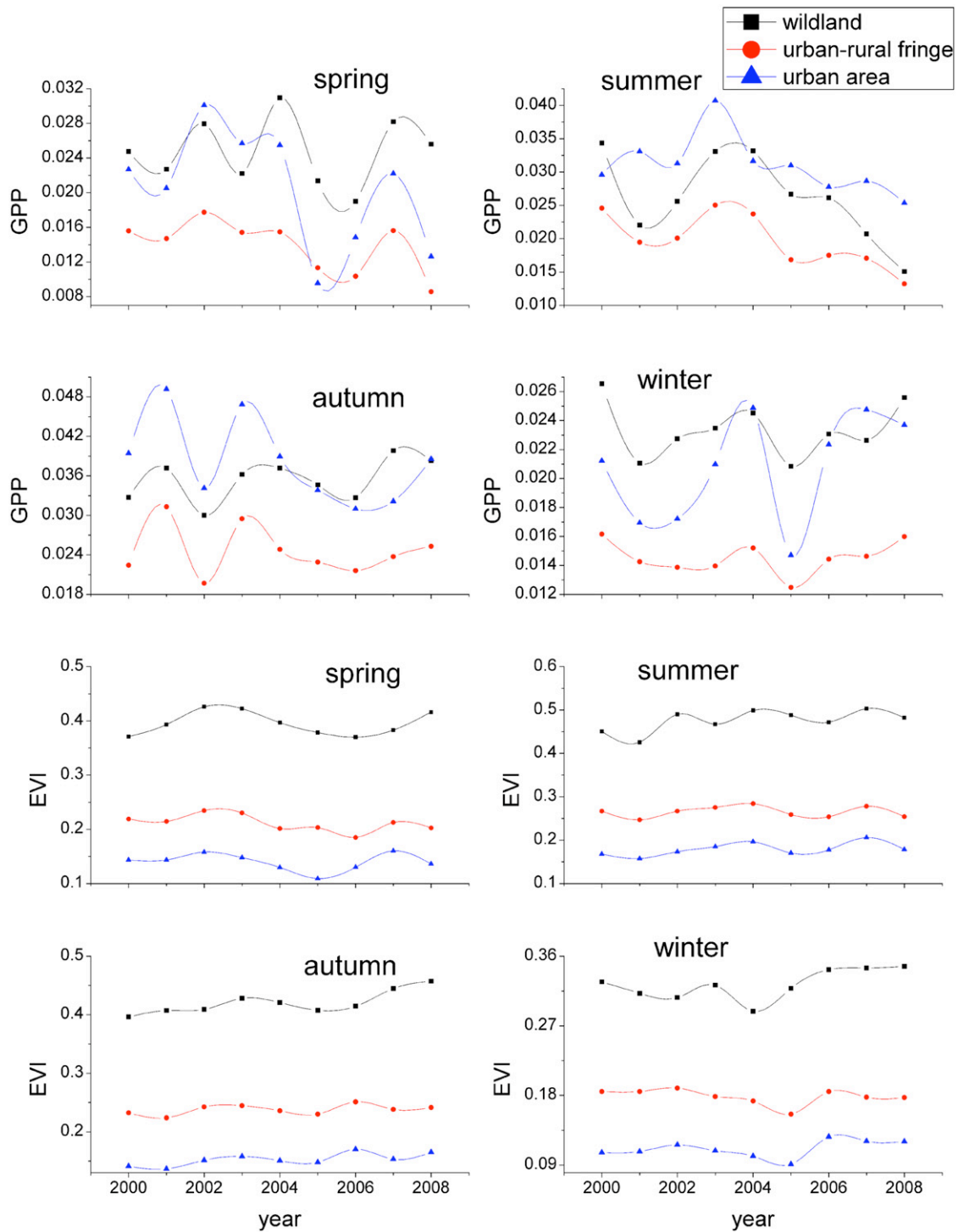
Figure 9. The seasonal trends of GPP and EVI over the three zones (urban, urban–rural fringe and wildland) along the urban–wildland transect from 2000–2008 in Greater Guangzhou. The time series was derived and spatially/temporally averaged with MODIS GPP and EVI datasets.

3.3. Comparison between urban green and natural vegetation

Figure 9 shows the difference in vegetation greenness over the three zones. A gradient of vegetation cover was observed from urban to wildland. Lower EVI occurred in the urban area and lower GPP appeared in the urban–rural fringe with decreasing trends. The difference of GPP and EVI in urban and rural areas is largely caused by the fact that the landscape in the urban area is dominated by buildings with impervious land surfaces, the urban–rural fringe area is partly cropland, while the urban–wildland fringe is dramatically influenced by urbanization with the loss of large areas of cropland and woodland. In contrast, natural land shows enhanced vegetation activities from 2000–2008 with increasing EVI and GPP, except for the summer GPP where the fraction of photosynthetically active radiation decreased by 11%, as indicated in the MODIS fPAR datasets.

Table 1. Comparison of impact of human activity with EVI and GPP.

| Zones | EVI[a] | GPP[a] | Impact of human activity[b] | |
			Scope	Intensity
Wildland	0.59	0.028	0	0
Urban–rural fringe	0.36	0.019	0.45	0.17
Urban	0.25	0.029	0.9	0.06

[a] Derived by using the MVC method in 2000 from MODIS EVI and GPP datasets; JJA EVI and GPP were spatially averaged through three zones.
[b] Impact of human activity was defined as urban expansion rate by using the percentage of built-up fraction to total land use fraction in 2000 over three zones.

Human activity around the mega-city area apparently modified land surface properties by converting cropland and natural forest to concrete and urban green that resulted in a net loss of green vegetation cover in most cases. In our study, photosynthesis intensity of vegetation was negatively related to the human-influenced gradient (table 1). The vegetation activity was enhanced under natural conditions (figure 6). However, pronounced decreasing trends happened in the urban–rural fringe area on expansion of urban to suburban areas with dramatic changes of land surface (figure 9) because spatially averaged change intensity of anthropogenic influence (table 1) in this area (0.17) was much greater than in the urban area (0.06) and wildland. The scope of the built-up change of this area also shows that about half of the former urban–rural fringe area was turned into non-vegetated land. Vegetation variation over the urban area from 2000–2008 may be a combined effect of human activity and climate change because temperature increases promote the photosynthetic activity of vegetation and city green is partially a result of human management.

The patterns of anthropogenic influence on vegetation in the mega-city area over the three zones were examined to quantify the vegetation growth influenced by historical human activities. First, we quantified the responding patterns of vegetation to land use and found that the order of vegetation cover change corresponding to land use was woodland > grassland > cropland > unused land > built-up > water body (figure 10). Water body had the lowest values due to no obvious beach vegetation cover across the study area. Built-up (mean EVI 0.27) had low vegetation cover due to the original vegetation cover being turned into urban landscape. Woodland had the higher vegetation cover due to its secondary or plantation wood vegetation. Vegetation cover of cropland showed seasonal variation.

4. Conclusions

This study demonstrated the vegetation activities over three sections along an urban–wildland transect in a subtropical region from 2000–2008 by examining EVI and GPP datasets from MODIS onboard Terra. Our results show that the photosynthetic activity of vegetation under natural conditions became stronger, but significantly decreased in the urban–rural fringe, largely reflecting the dramatic urban expansion
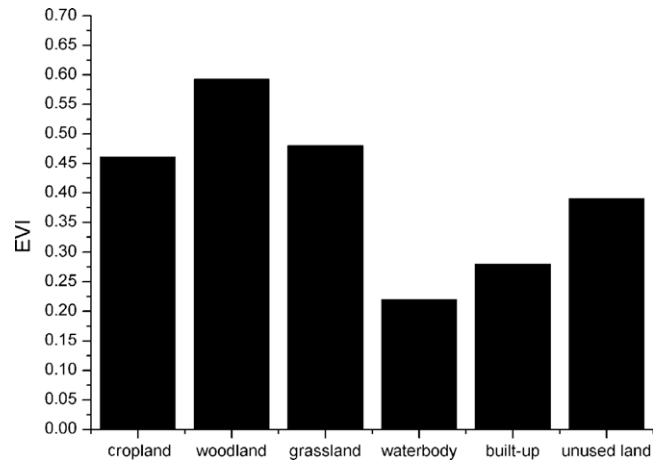
Figure 10. Average EVI value over different land use categories. Land use categories were considered to be different levels of human impact. Land use datasets of Greater Guangzhou in 2000 were combined with EVI processed with the MVC method to detect vegetation variation over different land use categories.

over the period. Meanwhile, a slight increase in vegetation greenness over urban areas may be a combined result of urban green management and climate change. The variability of surface temperature and solar radiance contributed to vegetation growth more than precipitation, indicating a positive response of vegetation to warming even in this southern subtropical region. The result was consistent with vegetation greening of the northern hemisphere during the last few decades over wildland. However, the dramatic decline of vegetation greenness in areas with large scale urbanization may not simply be considered as a local phenomenon. In a mega-city area like Greater Guangzhou, such a vegetation change may have climate implications at not only the local scale but also the regional scale.

Combinations of climate change and human activities have led to complex changes of vegetation production along the urban–wildland interface. Those changes in vegetation will, in turn, likely alter the heat-energy balance between land surface and atmosphere through modifying key land surface parameters, such as albedo and roughness. Large-scale changes of land surface conditions alter biophysical and biogeochemical processes that are important for atmospheric conditions and regional climate. The local climate over Greater Guangzhou may also be influenced by vegetation cover change. With the decrease of vegetation cover resulting from urbanization, urban heat islands will likely be intensified at the local, even regional, scales.

Acknowledgments

References

Braswell B H, Schimel D S, Linder E and Moore B 1997 The
    response of global terrestrial ecosystems to interannual
    temperature variability *Science* **278** 870–2
Buyantuyev A and Wu J 2009 Urbanization alters spatiotemporal
    patterns of ecosystem primary production: a case study of the
    Phoenix metropolitan region USA *J. Arid. Environ.* **73** 512–20
Cao M K and Woodward F I 1998 Dynamic responses of terrestrial
    ecosystem carbon cycling to global climate change *Nature*
    393 249–52
Chapin F S *et al* 2005 Role of land-surface changes in Arctic
    summer warming *Science* **310** 657–60
Dekker S C, Rietkerk M and Bierkens M 2007 Coupling microscale
    vegetation-soil water and macroscale vegetation-precipitation
    feedbacks in semiarid ecosystems *Global Change Biol.*
    13 671–8
Del Grosso S 2008 Global potential net primary production predicted
    from vegetation class, precipitation, and temperature *Ecology*
    89 2117–26
Doney S C and Schimel D S 2007 Carbon and climate system
    coupling on timescales from the Precambrian to the
    anthropocene *Ann. Rev. Environ. Resour.* **32** 31–66
Feddema J J, Oleson K W, Bonan G B, Mearns L O, Buja L E,
    Meehl G A and Washington W M 2005 The importance of
    land-cover change in simulating future climates *Science*
    310 1674–8
Foley J A *et al* 2005 Global consequences of land use *Science*
    309 570–4
Grimm N B, Faeth S H, Golubiewski N E, Redman C L, Wu J G,
    Bai X M and Briggs J M 2008 Global change and the ecology
    of cities *Science* **319** 756–60
Huete A, Didan K, Miura T, Rodriguez E P, Gao X and
    Ferreira L G 2002 Overview of the radiometric and biophysical
    performance of the MODIS vegetation indices *Remote Sens.
    Environ.* **83** 195–213
Huete A R, Didan K, Shimabukuro Y E, Ratana P, Saleska S R,
    Hutyra L R, Yang W Z, Nemani R R and Myneni R 2006
    Amazon rainforests green-up with sunlight in dry season
    Geophys. Res. Lett. **33** L06405

Kaufmann R K, Seto K C, Schneider A, Liu Z T, Zhou L M and
    Wang W L 2007 Climate response to rapid urban growth:
    evidence of a human-induced precipitation deficit *J. Clim.*
    20 2299–306
Kropelin S *et al* 2008 Climate-driven ecosystem succession in the
    Sahara: the past 6000 years *Science* **320** 765–8
Lin W S, Sui C H, Yang L M, Wang X M, Deng R R, Fani S J,
    Wu C S, Wang A Y, Fong S K and Lin H 2007 A numerical
    study of the influence of urban expansion on monthly climate in
    dry autumn over the Pearl River Delta, China *Theor. Appl.
    Climatol.* **89** 63–72
Myneni R B, Hall F G, Sellers P J and Marshak A L 1995 The
    interpretation of spectral vegetation indexes *IEEE Trans.
    Geosci. Remote* **33** 481–6
Myneni R B, Keeling C D, Tucker C J, Asrar G and Nemani R R
    1997 Increased plant growth in the northern high latitudes from
    1981 to 1991 *Nature* **386** 698–702
Pereira A R and Pruitt W O 2004 Adaptation of the Thornthwaite
    scheme for estimating daily reference evapotranspiration *Agr.
    Water Manag.* **66** 251–7
Taha H 1997 Urban climates and heat islands: albedo,
    evapotranspiration, and anthropogenic heat *Energ. Build.*
    25 99–103
Teixeira A, Bastiaanssen W, Ahmad M D, Moura M and Bos M G
    2008 Analysis of energy fluxes and vegetation-atmosphere
    parameters in irrigated and natural ecosystems of semi-arid
    Brazil *J. Hydrol.* **362** 110–27
Thornthwaite C W 1948 An approach toward a rational classification
    of climate *Geogr. Rev.* **38** 55–94
Trusilova K, Jung M and Churkina G 2009 On climate impacts of a
    potential expansion of urban land in Europe *J. Appl. Meteorol.
    Clim.* **48** 1971–80
Weng Q H 2001 Modeling urban growth effects on surface runoff
    with the integration of remote sensing and GIS *Environ. Manag.*
    28 737–48
Woodward F I, Lomas M R and Kelly C K 2004 Global climate and
    the distribution of plant biomes *Phil. Trans. R. Soc.* B
    359 1465–76
Woodward F I and Williams B G 1987 Climate and plant-distribution
    at global and local scales *Vegetation* **69** 189–97